JOURNAL OF GEOPHYSICAL RESEARCH, VOL. 114, A12215, doi:10.1029/2009JA014670, 2009

Proton aurora related to intervals of pulsations of diminishing periods

A. G. Yahnin,[1] T. A. Yahnina,[1] H. U. Frey,[2] T. Bösinger,[3] and J. Manninen[4]

Received 21 July 2009; accepted 2 September 2009; published 22 December 2009.

[1] Geomagnetic pulsations in the Pc1 frequency range are believed to be an indicator of electromagnetic ion cyclotron waves arriving from the equatorial magnetosphere, where the waves are generated because of a cyclotron instability of the anisotropic distribution of ring current ions. Proton precipitation produced by the cyclotron instability can be responsible for proton aurora. Indeed, the relationship between some types of proton aurora (proton spots and proton flashes) and pulsations in the Pc1 range (quasi-monochromatic Pc1 and Pc1 bursts) has already been found. The aim of this study is to find the proton aurora pattern, which relates to the kind of geomagnetic pulsations in the Pc1 range called intervals of pulsation of diminishing periods (IPDP). This is done on the basis of 2 year observations of geomagnetic pulsations at the Finnish meridional network of search coil magnetometers and proton aurora from the IMAGE spacecraft. We found that during IPDP the proton arcs appear equatorward of the proton oval at the meridian of the ground magnetometers. The maximum intensity of the pulsations is observed at the ground station, which is closest to the proton arc. The proton arcs tend to appear at lower latitudes at later magnetic local times (MLTs). This agrees with the facts that the IPDP occurrence exhibits a similar behavior and that the IPDP end frequency tends to increase with increasing MLT. In addition, data from geosynchronous spacecraft showed that IPDP occur when clouds of energy-dispersed energetic protons pass through the meridian of the ground magnetometers. The spatial-temporal correlation of IPDP with proton aurora arcs confirms the expectation that the proton arcs, like the proton spots and flashes, are the ionospheric image of the region where the ion cyclotron instability develops in the equatorial magnetosphere. In the case of IPDP the instability develops when drifting proton clouds resulting from particle injections in the night sector contact the plasmaspheric plume onto which the proton arcs map.

Citation: Yahnin, A. G., T. A. Yahnina, H. U. Frey, T. Bösinger, and J. Manninen (2009), Proton aurora related to intervals of pulsations of diminishing periods, *J. Geophys. Res.*, *114*, A12215, doi:10.1029/2009JA014670.

1. Introduction

[2] Intervals of pulsations of diminishing periods (IPDP) are geomagnetic pulsations in the Pc1–Pc2 range. Comprehensive descriptions of the IPDP morphology and hypotheses of the IPDP generation can be found in a review by *Kangas et al.* [1998, and references therein]. Although the investigation of IPDP has a rather long history, there is no clear understanding of specific features of these pulsations, including the formation of their dynamic spectra characterized by the frequency increase with time. Since the early stage of the IPDP investigation, it is generally accepted that the ground IPDP are the signature of electromagnetic ion cyclotron (EMIC) waves generated in the vicinity of the magnetospheric equatorial plane as a result of the ion cyclotron instability of ring current ions [e.g., *Troitskaya et al.*, 1968; *Fukunishi*, 1969; *Gendrin*, 1970; *Lin and Parks*, 1976]. This, in particular, suggests that IPDP may play a role in the dynamics of the ring current via pitch angle scattering of hot ions and, as a consequence, their precipitation and loss in the atmosphere.

[3] Proton precipitations related to IPDP were first observed by *Søraas et al.* [1980] on the basis of data from the low-orbiting ESRO satellite. *Yahnina et al.* [2003], using data from low-orbiting NOAA satellites, statistically established a relationship between IPDP and localized precipitation of energetic protons (LPEP) equatorward of the proton isotropy boundary (their type 2 LPEP). One may expect that this precipitation will produce a so-called proton aurora, which is the Doppler-shifted emission of neutral hydrogen atoms originating from precipitating protons after charge exchange.

[4] Observations with the FUV instrument on board the IMAGE spacecraft provided an excellent view of proton

[1]Polar Geophysical Institute, Kola Science Centre, Russian Academy of Science, Apatity, Russia.
[2]Space Sciences Laboratory, University of California, Berkeley, California, USA.
[3]Department of Physical Sciences, University of Oulu, Oulu, Finland.
[4]Sodankylä Geophysical Observatory, Sodankylä, Finland.

0148-0227/09/2009JA014670$09.00

Table 1. List of Ground Stations

Station	Station Abbreviation	Geographic Coordinates (deg)		Corrected Geomagnetic Coordinates (deg)		L Value
		Latitude	Longitude	Latitude	Longitude	
Kilpisjarvi	KIL	69.0	20.9	65.9	104.2	6.1
Ivalo	IVA	68.6	27.3	65.1	108.9	5.7
Sodankyla	SOD	67.4	26.4	64.0	107.4	5.3
Rovaniemi	ROV	66.8	25.9	63.6	106.6	5.1
Oulu	OUL	65.1	25.9	61.7	105.6	4.5
Nurmijarvi	NUR	60.5	24.6	56.9	102.4	3.4

auroras from space [*Frey*, 2007]. Different kinds of proton auroras were discovered equatorward from the main proton auroral oval. Some of these auroras have been correlated with geomagnetic pulsations of the Pc1 range and EMIC waves in space. *Yahnin et al.* [2007, 2008] showed that the subauroral proton spots, first described by *Frey et al.* [2004], exhibit a very nice correlation with long-lasting quasi-monochromatic Pc1 (''pearls''). As demonstrated by *Yahnina et al.* [2008], proton aurora flashes on the dayside, associated with magnetospheric compressions due to solar wind dynamic pressure pulses [*Zhang et al.*, 2002; *Hubert et al.*, 2003], exhibit a close connection with Pc1 bursts (called ''hydromagnetic emission bursts'' by *Fukunishi et al.* [1981]) as well as with EMIC waves of similar characteristics [see also *Zhang et al.*, 2008]. A correlation between detached proton arcs in the evening sector [*Immel et al.*, 2002; *Burch et al.*, 2002] and waves of the Pc1 frequency range has been noted by *Immel et al.* [2005] and *Spasojević et al.* [2005].

[5] These observations confirm the suggestion that proton auroras located equatorward of the main oval (equatorward of the proton isotropy boundary) are indeed the result of wave-particle cyclotron interaction. Thus, these proton auroras ''visualize'' the ionospheric projection of magnetospheric domains where wave-particle interactions develop. Such visualization of the source makes clear some properties of the geomagnetic pulsations (localization, duration, and frequency variations). For example, a close association of the pearl pulsations with the proton spots means that the source of these emissions is fairly localized. At the same time, the rotation of the source with a corotation speed around the Earth along the same L shell together with the source lifetime (as deduced from the proton spot dynamics in the ionosphere) explain the stability of the Pc1 frequency and long duration of the pulsations as measured at conjugated ground stations [*Yahnin et al.*, 2007]. Similarly, the dynamics of the proton flashes in the ionosphere explain the parameters of the Pc1 bursts, including variations of the upper frequency and frequency dispersion in the bursts [*Yahnina et al.*, 2008]. Mapping of the proton spots and proton flashes [*Frey et al.*, 2004; *Fuselier et al.*, 2004] onto the magnetospheric equatorial plane demonstrates that different types of pulsations (evidently corresponding to different regimes of the cyclotron interaction) are generated in different magnetospheric domains. The spots map into the vicinity of the plasmapause, where the fraction of He+ ions in the cold plasma composition is nonnegligible. The flashes map outside the plasmasphere, where the fraction of He+ is negligible. This probably explains why the pearls and Pc1 bursts are typically observed at frequencies below and above the He+ gyrofrequency, respectively [e.g., *Hansen et al.*, 1995].

[6] Reverting to IPDP, it would be important to find the proton aurora pattern visualizing the IPDP source configuration and dynamics on the ionospheric ''screen'' (as was done for quasi-monochromatic Pc1 and Pc1 bursts). This is the aim of the present study. We attempt to correlate IPDP and proton auroras by comparing IPDP observed at the Finnish meridional chain of induction coil magnetometers with proton aurora observations from the IMAGE spacecraft. In addition, proton flux observations on board NOAA Polar Operational Environmental Satellite (POES) and Los Alamos National Laboratory (LANL) spacecraft in the ionosphere and equatorial plane are used. In section 2 the data are briefly described. Section 3 presents the results. We start from a description of properties of IPDP revealed from the ground observations. Then, the IPDP–proton aurora relationship is considered on the basis of both case and statistical studies. The summary of the results is given in section 4. The discussion and conclusions are presented in sections 5 and 6, respectively.

2. Data

[7] The ground observations of geomagnetic pulsations were performed by the Finnish network of search coil magnetometers located at corrected geomagnetic latitudes (CGLAT) 56.9°–65.1° and MLT = UT + 2 (see Table 1). The magnetometers of the Finnish chain have the same linear frequency response of 1.4 V/(nT × Hz) with an instrumental noise figure of ~1 pT/Hz$^{1/2}$ at 1 Hz. The magnetometers of the Finnish network are identical and intercalibrated, so they can be used for the comparison of pulsation intensities at stations along the meridian.

[8] The proton aurora data were provided by the Spectrographic Imager (SI) of the FUV instrument on board the IMAGE spacecraft (see *Mende et al.* [2000] for details), which was designed to select the Doppler-shifted Lyman H alpha line at 121.82 nm and to reject the non-Doppler-shifted Lyman H alpha from the geocorona at 121.567 nm. Another detector, the Wideband Imaging Camera (WIC), selects the spectral range between 140 and 180 nm in the ultraviolet part of the optical spectrum, mostly detecting nitrogen Lyman-Birge-Hopfield bands and atomic lines. Precipitating protons can also contribute to the WIC measurements along with electrons [*Frey et al.*, 2003].

[9] Additionally, data from the medium energy proton and electron detector (MEPED) and total energy detector (TED) instruments on board the low-orbiting NOAA POES satellites, measuring particles with energies $E > 30$ keV and

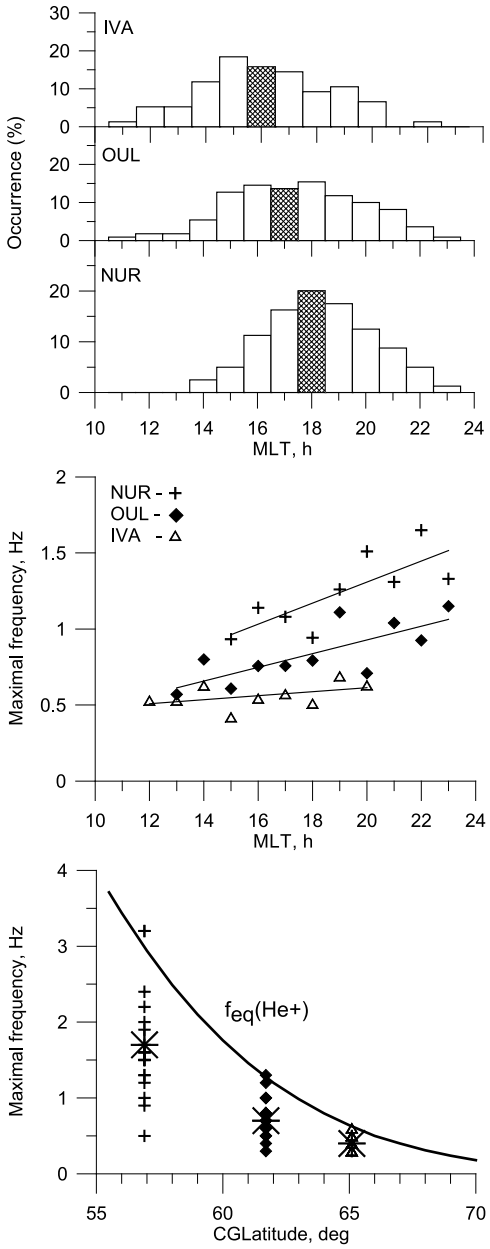

Figure 1. Statistical properties of IPDP as derived from observations by the Finnish network of pulsation magnetometers. (top) MLT distribution of the IPDP occurrence at stations IVA, OUL, and NUR. Hatched columns indicate medians of distributions. (middle) Dependence on MLT of the hourly average end frequency of IPDP as observed at IVA, OUL, and NUR. (bottom) Dependence of the He+ gyrofrequency on the distance from the Earth in the equatorial plane of the magnetosphere (thick line) and the IPDP end frequencies as observed at IVA, OUL, and NUR for those cases when IPDP were observed only at one station. Asterisks mark median values of the end frequencies.

E < 20 keV, respectively [*Evans and Greer*, 2000], were used to identify the particles responsible for the aurora. The satellites of the NOAA POES series have polar circular orbits at altitudes around 800 km. The MEPED instrument measures energetic protons with two solid-state detector telescopes. The NOAA satellites are three-axis stabilized, and one detector views along the Earth-satellite radial vector. At high latitudes (L > 3) the detector viewing along this direction measures particles within the loss cone. The second detector views perpendicularly to the Earth-satellite vector. It observes particles that will magnetically mirror above the atmosphere. The TED instrument measures the total energy flux of particles within the loss cone at high latitudes.

[10] Up to five LANL geosynchronous satellites monitored the charged particles during the time interval under study. They were equipped, in particular, with the Synchronous Orbit Particle Analyzer (SOPA) [*Belian et al.*, 1992], which can measure particles with energies of more than 50 keV. For the aims of this study the data from five "low-energy" proton detectors measuring the particles in the energy ranges of 50–75, 75–113, 113–170, 170–250, and 250–400 keV are used.

3. Results

3.1. Event Selection

[11] Data for the years 2004 and 2005 were used for this study. First, the data from three stations, IVA, OUL, and NUR (representing poleward, middle, and equatorward parts of the magnetometer chain, respectively), were searched to reveal IPDP events observed at at least one station. In all, 153 events were found (74 events in 2004 and 79 events in 2005). For all events the IPDP beginning and ending times were determined as well as the end frequency. Then, those events were selected when observations of proton aurora from the IMAGE spacecraft were available (35 events, 9 in 2004 and 26 in 2005).

3.2. Some Statistical Properties of IPDP

[12] All the IPDP events were found within 12–23 MLT (some 80% of events were within 15–21 MLT). Sixty-three of 153 events were observed at only one station (22, 20, and 21 in IVA, OUL, and NUR, respectively). Note that observation of the signal at only one station suggests the close location of the IPDP ionospheric source. Twenty-five events were observed simultaneously at all three stations. Other IPDP events were observed simultaneously at two neighboring stations: at IVA and OUL (30 events) or OUL and NUR (35 events). The number of events registered in IVA, OUL, and NUR was 76, 110, and 81, respectively.

[13] In Figure 1 (top) the occurrence of IPDP events relative to MLT for each of the three stations is shown. The medians of distributions fall at 16, 17, and 18 MLT for IVA, OUL, and NUR, respectively. Thus, the station at lower latitude observes IPDP at later MLT. A similar dependence had been noted by *Søraas et al.* [1980]. We also investigated the dependence of the IPDP end frequency on MLT. The dependencies of the average (over 1 h of MLT) values of the end frequency for each of the three stations are presented in Figure 1 (middle). The end frequency increases with MLT at every station. Figure 1 (middle) shows that at any MLT the averaged end frequency depends on latitude. The higher the latitude of a station, the lower is the averaged IPDP end frequency. The dependence on latitude is also seen in Figure 1 (bottom), where the end

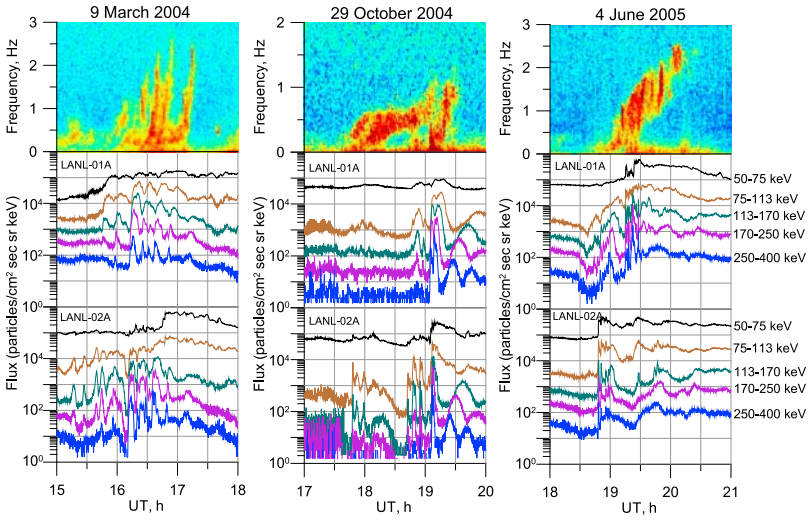

Figure 2. (top) Examples of the IPDP events along with (middle and bottom) the data from two geosynchronous spacecraft whose meridians are astride the meridian of the ground pulsation observations.

frequencies are plotted for those 63 IPDP events which were observed only at one of the three stations. In Figure 1 (bottom), the equatorial He+ gyrofrequency (in the dipole magnetic field) is also shown. Almost all observed end frequencies are below the He+ gyrofrequency. This agrees with earlier findings [see *Pikkarainen et al.*, 1983]. In our approach, however, we should note that the end frequency is determined for the sources located close to the observing ground station. Both dependencies of the IPDP frequency on latitude and the He+ frequency are consistent with the concept that IPDP represent ion cyclotron waves.

3.3. Relationship of IPDP, Proton Aurora, and Proton Injection

3.3.1. Event of 9 March 2004

[14] On 9 March 2004 a series of IPDP was observed at 1550–1715 UT (Figure 2, left). The end frequencies in this series reached more than 2 Hz. Let us consider phenomena related to the last IPDP event in this series at 1650–1715 UT. During this IPDP, the IMAGE spacecraft observed a distinct proton arc appearing in the evening sector. The development of this arc is shown in a sequence of proton aurora images in Figure 3. The arc became distinguishable from the proton oval at 1656 UT, and it was seen until 1712 UT. During the arc's lifetime, it shifted equatorward slightly (for about 2°–3°). The arc crossed the meridian of the ground network close to the latitude of the ground station NUR. The most intense IPDP signal was observed right at this station. The intensity sharply decreased with latitude; the pulsations were hardly seen in ROV and were not seen poleward of it.

[15] The proton arc in Figure 3 is clearly seen in the late evening sector, but toward earlier MLT it is juxtaposed with the proton oval and, consequently, it is hardly resolved in the images. The existence of the arc at 18 MLT is confirmed by the particle data from the NOAA satellite that crosses this region at ~1705 UT. These data demonstrate a LPEP equatorward of the precipitation related to the proton oval (Figure 4, top). Such a precipitation pattern has been found by *Yahnina et al.* [2003] as being closely related to EMIC waves. (We should note that the proton aurora images were obtained in the Southern Hemisphere, while the ground-based and NOAA observations were made in the Northern Hemisphere. The interhemispheric mapping was done using the International Geomagnetic Reference Field model, IGRF-10.)

[16] Data from two geosynchronous spacecraft (LANL 01A and 02A), whose longitudes (7.8°E and 69.8°E,

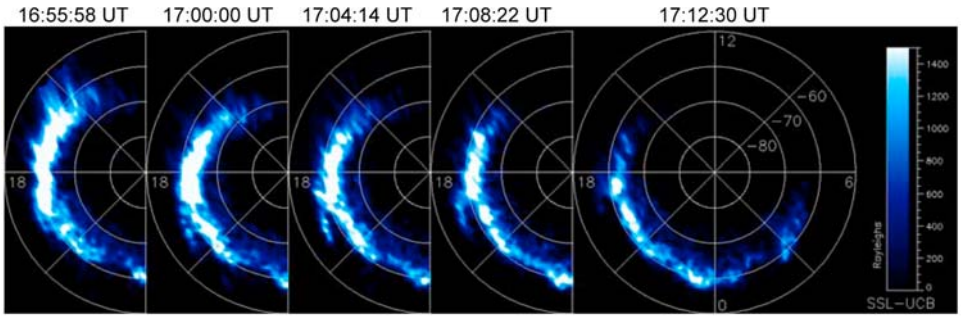

Figure 3. Sequence of images of the proton aurora from the IMAGE spacecraft for the interval of 1656–1712 UT on 9 March 2004.

respectively) are astride the magnetometer chain, show multiple injections of the energetic protons on the nightside and subsequent westward drift of the proton clouds. The drift is evidenced by the systematic delay of the flux enhancements at LANL 01A in comparison to LANL 02A and by the energy dispersion, which is more pronounced at LANL 01A. The higher-energy protons arrive first, and lower-energy protons are delayed because of the fact that the azimuthal drift velocity is proportional to the particle energy. The spacecraft LANL 01A was situated about 1.5 h MLT westward of the ground magnetometer network observing IPDP, while the spacecraft LANL 02A was about 2.5 h eastward from the network. Figure 2 shows remarkable correlations between energy-dispersed increases of the energetic proton flux registered on board spacecraft LANL 01A (closest to the meridian of magnetometers) and IPDP observed on the ground.

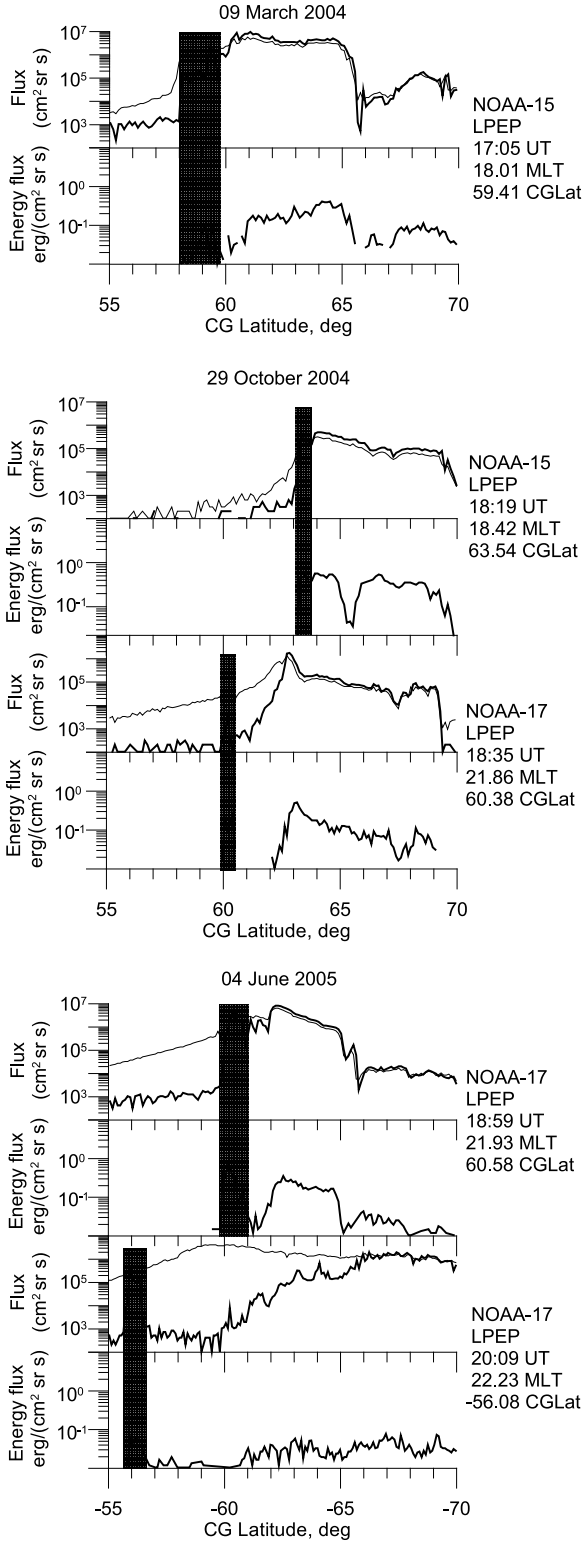

Figure 4. The NOAA POES proton measurements during the IPDP events presented in Figure 2. (top) Latitudinal profiles of the proton flux in the energy range 30–80 keV and total energy flux of protons with $E < 20$ keV from the MEPED and TED instruments on board the NOAA 15 satellite during the IPDP event on 9 March 2004. Thick (thin) line shows the precipitating (trapped) flux. The vertical strip indicates the LPEP location. The legend on the right presents UT, MLT, and CGLAT of the LPEP maximum. (middle) The same as Figure 4 (top), except for NOAA 15 and NOAA 17 observing LPEP at close times and at different locations during the IPDP event on 29 October 2004. (bottom) The same as Figure 4 (top), except for NOAA 17 observing LPEP at the beginning and end of the IPDP event on 4 June 2005.

3.3.2. Event of 29 October 2004

[17] A series of IPDP was observed between 1750 and 1930 UT on 29 October 2004 (Figure 5). Let us concentrate on phenomena related to the IPDP event at ~1800–1830 UT, when the IPDP end frequency reached ~0.7 Hz. In Figure 5 one of the SI12 images obtained during this event is also presented. The vertical line in the spectrogram stack plot marks the time (~1816 UT) when this proton aurora display was obtained. One may see the proton arc, which crossed the meridian of the ground stations (~20.3 MLT). The arc was observed at 1755–1836 UT and occupied the 18–22 MLT sector. The arc location is confirmed by particle measurements of the NOAA 15 and 17 satellites (Figure 4, middle). These satellites passed the evening sector arc at ~18.4 and ~21.9 MLT and at 1819 and 1835 UT, respectively. Although at these locations the arc was hardly distinguishable (because of juxtaposition with the proton oval at 18 MLT and because of weak intensity of the arc at ~22 MLT), both satellites observed LPEP (marked by triangles in Figure 5, right) equatorward of the proton oval. In Figure 5 (bottom right), the proton arc position at 1816 UT is also shown in rectangular coordinates along with locations of the ground stations. The station OUL, which observed the most intense pulsations, is the closest to the arc. The larger the latitudinal distance from the proton arc to a station, the weaker is the registered IPDP signal. Note that during this event the proton arc did not exhibit any significant latitudinal movement.

[18] Again, IPDP occur in accord with the injections of energetic protons registered at geosynchronous orbit (Figure 2, middle). The spacecraft LANL 02A observed dispersionless injections in the night sector (~22.5 MLT at 1800 UT) related to weak substorm activations (seen as auroral brightening around midnight in the WIC data, not shown). During IPDP the weak but clear dispersed injec-

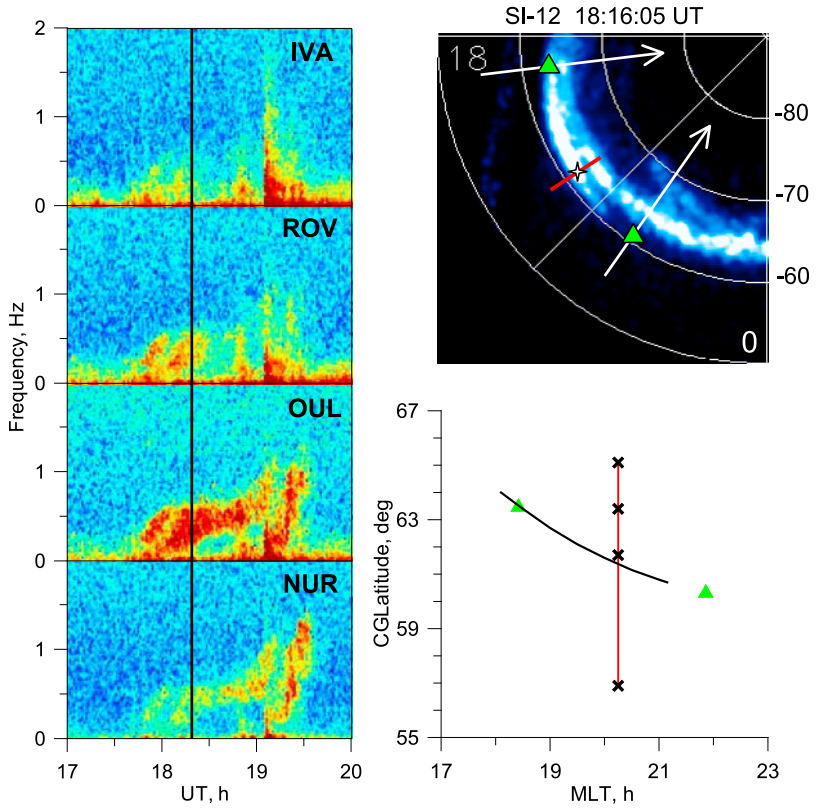

Figure 5. (left) Spectra of pulsations registered at four stations of the Finnish meridional network for the interval of 1700–2000 UT on 29 October 2004 and (top right) the proton aurora display from the IMAGE spacecraft made at ~1816 UT. Along with the proton aurora, the traces of two NOAA satellites (mapped from the Northern Hemisphere) are shown by white lines with arrows. Triangles mark the locations of LPEPs. The bar and star at ~20.3 MLT indicate the conjugated locations of the meridional magnetometer chain and station OUL, respectively. (bottom right) The locations of the proton arc and ground stations in rectangular coordinates are also shown.

tions were seen at LANL 01A (~18.5 MLT), which is closest to the meridian of the magnetometer network.

3.3.3. Event of 4 June 2005

[19] An isolated IPDP event was registered at 1855–2015 UT on 4 June 2005 at station NUR (Figure 2, right). The end frequency of IPDP was 2.6 Hz. The signal was hardly distinguishable in OUL and was not seen poleward. The proton aurora data from IMAGE showed a clear signature of the proton arc only at 1926 UT (Figure 6). (It should be noted that the proton aurora image was cut off around 21 MLT during this interval.) However, the NOAA 17 satellite registered LPEP above the region adjoining the equatorial boundary of the proton oval at about 22 MLT as early as 1859 UT (Figure 4, bottom). This likely means that the arc was simply not resolved by the SI12 instrument at that time. Indeed, since 1903 UT the suboval arc is already clearly seen in the data of the IMAGE WIC (Figure 6) in the location conjugated with LPEP. The WIC can observe the emissions related to both electron and proton precipitations [e.g., *Frey et al.*, 2003]. One can realize that this suboval arc is produced by the proton precipitation since NOAA 17 did not observe any significant flux of auroral electrons in conjunction with LPEP (data not shown). Unfortunately, we cannot compare the times of the IPDP end and proton arc decay because the optical data are not available after 1934 UT. Between 1903 and 1934 UT the proton arc shifted toward the equator for about 2° (from CGLAT ~−60° to ~−58°). During the next half hour the arc most likely shifted another 2°. This is evidenced by the NOAA 17 data, which show LPEP at CGLAT −56° at 2009 UT (Figure 4).

[20] This long-lasting IPDP event was also associated with proton injections registered by LANL spacecraft. The spacecraft LANL 02A (located at ~23.5 MLT) registered dispersionless pulsed proton injections related to the substorm activation developing near midnight. The proton cloud related to this injection is seen around 1900 UT at the location of LANL 01A (~19.5 MLT) as dispersed injection. New substorm activation occurred in the evening sector (as evidenced by the WIC data in Figure 6). The appearance of the auroral bulge around the meridian of LANL 01A is associated with the dispersionless injection at this location (at ~1915 UT). Further, the auroral bulge expanded from the evening to the night sector, and the next injections were seen at both the 01A and 02A spacecraft. Thus, during this event the geosynchronous spacecraft LANL 01A, which is the closest to the meridian of ground magnetometers, observed both dispersed and dispersionless injections.

3.4. Statistics of the Relationship Between IPDP, Proton Arcs, and Proton Injections

[21] The three events considered above show that IPDP relate to the appearance of suboval proton arcs and drifting

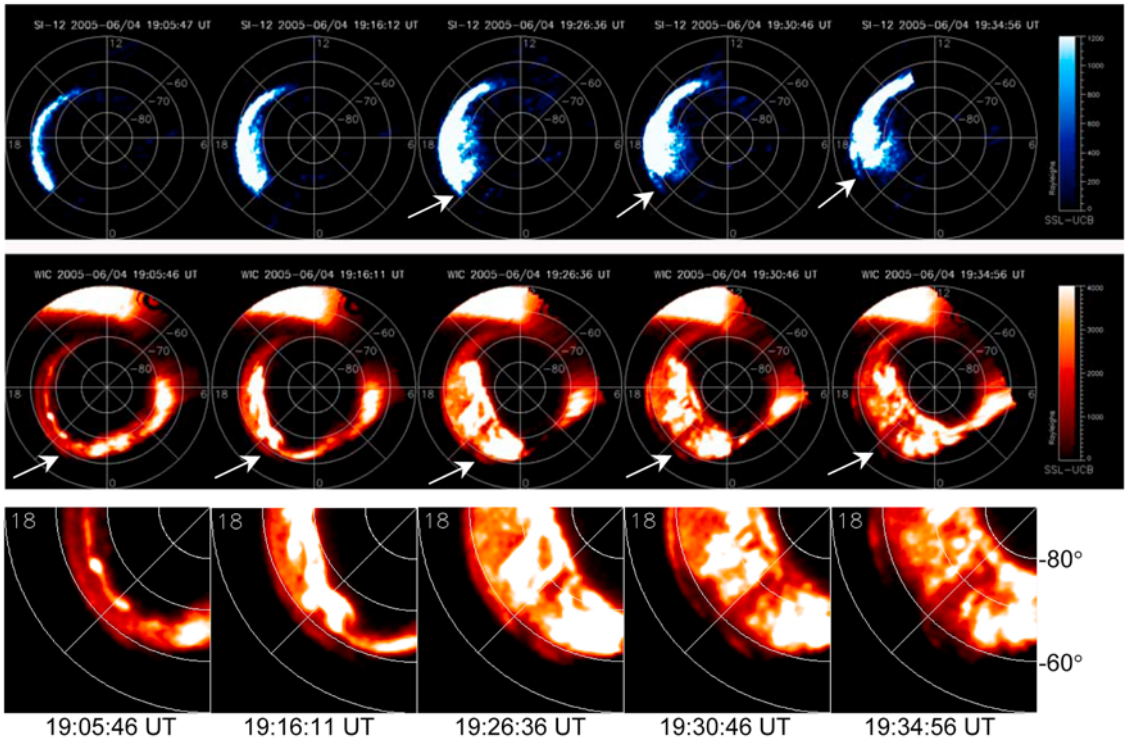

Figure 6. Selected auroral images from the IMAGE spacecraft made during the interval 1905–1935 UT on 4 June 2005. (top) The SI12 images are shown. (middle) The WIC images show the development of the auroral substorm. Arrows point to the suboval proton arc. (bottom) Enlarged fragments of the WIC images show the suboval arc and its dynamics more clearly.

proton clouds. Consideration of all 35 events, when proton aurora observations were available during IPDP events, confirmed this relationship. Indeed, in 30 cases the IPDP observations were associated with clear signatures of the proton arc appearance in the vicinity of the ground stations. The proton arcs became visible and disappeared within a few minutes of the IPDP start and end, respectively. The proton arcs were observed in the latitudinal range of 53°–66° CGLAT and exhibited a clear tendency to appear at lower latitudes at later MLTs. This is, evidently, a consequence of the configuration in the evening sector of the proton oval, whose equatorial boundary, representing the proton isotropy boundary, shifts equatorward from day to late evening. The locations of the proton arcs in MLT-CGLAT coordinates are shown in Figure 7. Among 63 events, when IPDP were observed at only one of the three selected stations (see section 3.2), the observations of proton aurora arcs were available in 15 cases. Three such IPDP were observed in IVA, six in OUL, and six in NUR. The latitudinal locations of the arcs associated with IPDP observed only in IVA, OUL, and NUR were within 64°–66°, 60°–63°, and 53°–58° CGLAT, respectively, that is, close to the IPDP observing station. These arcs were observed at 12.5–14.5 MLT, 15.5–22 MLT, and 19–22.5 MLT, respectively.

[22] Most arcs exhibited a drift toward low latitudes as in the examples presented in sections 3.3.1 and 3.3.3. Typically, the equatorward shift was not large and amounted to 1°–3°. The largest shift of the proton arc was observed during an IPDP event at 1800–1900 UT on 12 June 2005 (data not shown); it was as large as ~6°. Some proton arcs were, in contrast, immovable like that in section 3.3.2.

[23] For 28 of 30 proton arc observations, there exist NOAA POES passes, which crossed the proton arcs. The data from all these NOAA passes show the presence of LPEP in conjunction with the arc. During four of five

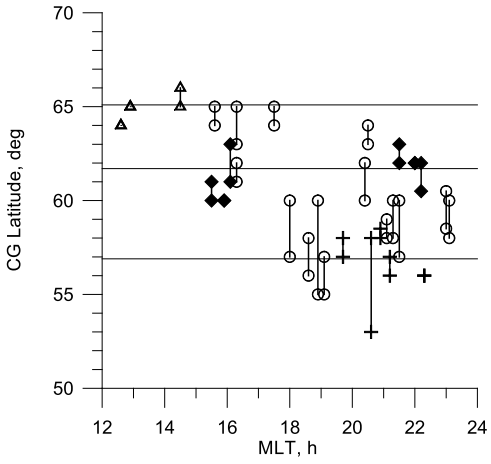

Figure 7. The latitudinal locations of the suboval proton arc related to the IPDP events in 2004–2005. The vertical bars indicate the latitudinal shift during the arc lifetime at the longitude of the ground magnetometer network. Triangles, squares, and crosses mark those arcs that occurred during IPDP events registered only at IVA, OUL, and NUR, respectively. Circles mark other arcs.

events, when the arc was not seen on proton aurora images, there were fortunate passes of NOAA POES close to locations of the ground station observing IPDP. The particle data from these passes also showed the presence of LPEP adjoining (from the equatorial side) the region of isotropic proton fluxes and conjugated with the equatorward part of the proton aurora oval. Evidently, in these cases the arcs were either too dim and below the sensitivity threshold or simply were not resolved from the oval on the images.

[24] In 34 of 35 cases of proton aurora observations the data from geosynchronous LANL spacecraft situated in the evening sector were available. In all these cases the data showed injections of hot protons during the IPDP events. In particular, the data from the spacecraft LANL 01A were available in 33 cases. In all of these 33 cases the injections observed on board LANL 01A exhibited good temporal correlation with IPDP, as shown in sections 3.3.1–3.3.3.

4. Summary

[25] Our data can be summarized into three major observations.

[26] 1. Consideration of peculiarities of geomagnetic pulsations of the IPDP type observed during 2 years at the meridional network of search coil magnetometers showed that (1) IPDP tend to appear at lower latitudes at later MLTs; (2) the IPDP end frequency tends to increase when MLT increases; and (3) when IPDP were observed at only one of three selected stations (this suggests that the pulsation source footprint is close to this station), the IPDP end frequency was less than the equatorial gyrofrequency of He+.

[27] 2. Observations of the proton aurora from the IMAGE spacecraft during IPDP events showed that (1) during IPDP the suboval proton arcs appear at the meridian of the ground magnetometer network; (2) the maximal intensity of the pulsations is observed at the ground station which is closest to the proton arc; (3) the arcs' appearance and fading are within several minutes of the start and end of the IPDP events, respectively; and (4) the proton arcs tend to appear at lower latitudes at later MLTs.

[28] 3. The IPDP events correlate with energetic proton injections seen on the geosynchronous orbit close to the meridian of the IPDP observations.

5. Discussion

[29] The results listed above demonstrate the close spatial-temporal relationship between IPDP and proton arcs. This relationship confirms the suggestions about the ion cyclotron instability as a mechanism producing the proton precipitation responsible for the suboval proton arc in the evening sector [*Burch et al.*, 2002; *Immel et al.*, 2002; *Spasojević et al.*, 2004, 2005; *Jordanova et al.*, 2007]. Thus, the suboval proton arc represents the projection of the magnetospheric source region of the IPDP onto the ionosphere.

[30] In the evening sector the proton arcs tend to map onto the eastern edge of the plasmaspheric plume [*Spasojević et al.*, 2005; *Jordanova et al.*, 2007]. A close spatial-temporal association of IPDP and drifting proton clouds strongly suggests that the wave-particle interaction responsible for both proton precipitation and IPDP develops when drift trajectories of hot protons intersect the boundary of the cold plasma represented by the plasmaspheric plume. This agrees with a current scenario suggesting ring current particle losses in the evening sector due to ion cyclotron wave-particle interaction [*Bespalov et al.*, 1994; *Trakhtengerts and Demekhov*, 2005; *Kozyra et al.*, 1997; *Khazanov et al.*, 2007]. Recently, *Jordanova et al.* [2007] performed a numerical modeling of two particular events of proton arc observations on the basis of their global ring current–atmosphere interactions model. It includes the cyclotron wave interaction with hot protons. Their modeling reproduced reasonably well the proton precipitation resembling the observed proton arc being extended along the eastern boundary of the plasmaspheric plume.

[31] Typically, the proton arc extends from higher latitudes at earlier MLT to lower latitudes at later MLT. This agrees with the plasmaspheric plume extension to larger distance from the Earth on the dayside in comparison with that in the evening sector.

[32] The morphology of the proton arcs explains the MLT dependence of the IPDP occurrence at these stations as shown in Figure 1. Keeping in mind the range of latitudinal locations of proton arcs, it is clear that the IPDP signal arriving from the high-latitudinal part of the dayside source region is more distinguishable at the higher-latitude ground stations (e.g., IVA). The most equatorward station (NUR) is better for discerning the signal from the low-latitudinal part of the source region, which is located in the evening side. (The signal from a remote source suffers attenuation when propagating in the ionospheric waveguide. Previous studies of the relationship between suboval proton aurora and pulsations in the Pc1 range [*Yahnin et al.*, 2007, 2008; *Yahnina et al.*, 2008] have undoubtedly demonstrated the significance of wave attenuation off the proton aurora location.) The decrease of the latitude of the IPDP source region toward later MLTs also agrees with the general trend of the end frequency of IPDP to increase from day to late evening local times (Figure 1). Different dependencies for given stations are due to the fact that the main contribution to the average end frequency comes from those sources whose footprints (proton arcs) are located closer to the observation site.

[33] *Immel et al.* [2005] compared the proton arcs and ground observations of geomagnetic pulsations in the Pc1 range. They found a distinct association of the arcs with Pc1 waves in three of four cases (note that in the exceptional case the ground stations were situated outside the proton arc, so the lack of Pc1 signal could be caused by the wave's attenuation in the ionospheric waveguide). One of the pulsation events in the study by Immel et al. can be interpreted as IPDP, and two others can be classified as quasi-monochromatic Pc1. This does not contradict with our findings because in our study we looked for proton aurora signatures in relation to IPDP while Immel et al. focused on the proton arcs and looked for any kind of associated pulsations. Both Immel et al.'s and our findings are in agreement with results by *Yahnina et al.* [2003], who found that the LPEP events in the evening sector correlate with both IPDP and Pc1–Pc2 observed at the ground station nearby. The difference in dynamic spectra of the pulsations

is likely linked with different physical conditions in the source region. One can easily accept that steady conditions (e.g., a constant intensity of the hot particle flux at the cold plasma boundary) correspond to the generation of EMIC waves, which have steady characteristics (Pc1–Pc2). As for IPDP, their generation is undoubtedly linked with unsteady conditions since they do occur during the energy-dispersed enhancements of the proton flux within the drifting proton cloud.

[34] As has been noted in section 1, the exact mechanism of the IPDP spectra formation is still unclear. Control of the IPDP source on the basis of observations of the proton arcs can provide some constrains for this mechanism. For instance, one debatable view on the IPDP generation suggests that the increase of the frequency is due to the equatorward movement of the source [e.g., *Troitskaya et al.*, 1968; *Kiselev and Raspopov*, 1971; *Maltseva et al.*, 1981; *Baishev et al.*, 2000]. Indeed, often, but not always, the proton arcs move equatorward while IPDP develop. There is, however, discordance between the observed IPDP frequency range and that expected from the proton arc equatorward movement. In most cases the latitudinal shift of the arc was about 1°–3°. In the example from section 3.3.3 the arc appeared at about 1903 UT and was observable up to 1934 UT when the IMAGE observations were stopped. During this period the arc shifted equatorward for some 2° (from ~60° to 58°). In the dipole magnetic field this shift corresponds to a ratio in the IPDP frequencies of 1.4. Let us assume that the IPDP frequency is a fixed fraction of the equatorial He+ gyrofrequency. Since the IPDP frequency at 1934 UT was about 1.5 Hz, the frequency at 1903 UT should accordingly be about 1 Hz. In fact, it was about 0.1–0.2 Hz.

[35] During the "extreme" event at 1800–1900 UT of 12 June 2005 (data not shown) the IPDP end frequency was ~3 Hz, and the shift of the proton arc was as large as 6° (from 60° to 54°). According to the hypothesis of inward movement of the IPDP source, this should provide the increase of the pulsation frequency for ~2 times. Therefore, the start frequency should be about 1.5 Hz. In fact, the start frequency was again 0.1–0.2 Hz.

[36] Thus, although the inward motion of the IPDP source should give some contribution to the frequency growth, it is not enough to provide the frequency increase of a decade, as typically observed [e.g., *Heacock*, 1967; *Kangas et al.*, 1998]. Furthermore, the source does not necessarily move equatorward (see, for example, the event described in section 3.3.2).

[37] Another popular hypothesis explains the frequency growth with the energy dispersion of the longitudinally drifting hot protons [e.g., *Fukunishi*, 1969; *Lin and Parks*, 1976; *Maltseva et al.*, 1970]. According to this view the frequency growth relates to a gradual decrease of the energy of the resonant protons arriving at a given location. The close relationship between IPDP and (often dispersed) proton injections sustains this view.

[38] It is worth noting that the relationship was concluded from data of nonconjugated locations. Indeed, the injections were observed at L = 6.6 while the IPDP sources were at L ~ 3–5. This implies that the injections should have a large radial dimension. At the same time, this does not guarantee that the amplitude of the fast variations of the proton fluxes at deeper locations is always as distinct as at geosynchronous orbit. This could be the reason why in some cases the multiple injections correlate well with multiple IPDP (as in the case of 9 March 2004; see Figure 2) but in other cases relate to a single IPDP event (as in the case of 4 June 2005). In the later case, it appears that the IPDP correlate with the whole proton flux enhancement at LANL 01A rather than with separate injections. The whole proton enhancement exhibits a smoothening of the proton energy spectrum in the course of an IPDP event like that during a dispersed injection.

[39] To verify if the energy dispersion alone provides the observed frequency changes, one needs detailed in situ measurements of the energy spectrum and anisotropy of the injected protons as well as the ion composition and density of the cold plasma. It is most likely that the observed IPDP spectra are formed by a combination of the two above-mentioned mechanisms, although some other mechanisms were also proposed [e.g., *Kangas et al.*, 1998].

6. Conclusion

[40] On the basis of a comparison of ground magnetometer data with proton aurora observations from the IMAGE spacecraft, we explored the spatial-temporal correlation of geomagnetic pulsations called IPDP with proton aurora arcs observed equatorward of the proton oval. This confirms the suggestion that proton arcs are the result of the ion cyclotron instability developing in the equatorial plane of the magnetosphere. The instability develops when proton clouds resulting from particle injections in the night sector contact the plasmaspheric plume. The morphology of the proton arcs was found to be in tune with the statistical properties of IPDP. These findings provide some constraints for mechanisms of the IPDP spectra formation.

[41] Previous studies have established the connection between quasi-monochromatic Pc1 pulsations and Pc1 bursts with different forms of suboval proton aurora. In this paper such connection is also proved to exist for IPDP, which are another type of pulsations in the Pc1 range. All these pulsations represent different regimes of the ion cyclotron interaction in the near-Earth equatorial magnetosphere. Thus, the proton aurora observations represent the two-dimensional image of the interaction region at the ionosphere level and provide a powerful tool for monitoring and diagnosis of the cyclotron interaction regimes.

[42] **Acknowledgments.** The NOAA POES data were provided by NOAA. The energetic proton flux data were provided by the LANL energetic particle team. The study of T.A.Y. and A.G.Y. was performed in frames of the basic research program 16/3, "Solar activity and space weather," of the Presidium of the Russian Academy of Sciences (RAS) and program VI.15, "Plasma processes in the solar system," of the Division of Physical Sciences of the RAS. A.G.Y. thanks the Academy of Finland for support of the exchange visit to the University of Oulu in 2007 when this study was started. The work of H.U.F. was supported by NASA under award NNG05GF24G.

[43] Zuyin Pu thanks James Burch and Finn Søraas for their assistance in evaluating this paper.

References

Baishev, D. G., E. S. Barkova, S. I. Solovyev, K. Yumoto, and A. G. Yahnin (2000), Frequency growth of IPDPs during a substorm as a manifestation of equatorward expansion of particle precipitation and current region, *Int. J. Geomagn. Aeron.*, *2*, 115–127.

Belian, R. D., G. R. Gisler, T. Cayton, and R. Christensen (1992), High-*Z* energetic particles at geosynchronous orbit during the great solar proton

event series of October 1989, *J. Geophys. Res.*, *97*, 16,897–16,906, doi:10.1029/92JA01139.

Bespalov, P. A., A. G. Demekhov, A. Grafe, and V. Y. Trakhtengerts (1994), On the role of collective interaction in asymmetric ring current formation, *Ann. Geophys.*, *12*(5), 422–430, doi:10.1007/s00585-994-0422-8.

Burch, J. L., W. S. Lewis, T. J. Immel, P. C. Anderson, H. U. Frey, S. A. Fuselier, J.-C. Gérard, S. B. Mende, D. G. Mitchell, and M. F. Thorsen (2002), Interplanetary magnetic field control of afternoon-sector detached proton auroral arcs, *J. Geophys. Res.*, *107*(A9), 1251, doi:10.1029/2001JA007554.

Evans, D. S., and M. S. Greer (2000), Polar Orbiting Environmental Satellite Space Environment Monitor-2 instrument descriptions and archive data documentation, *Tech. Memo. OAR SEC-93*, NOAA, Boulder, Colo.

Frey, H. U. (2007), Localized aurora beyond the auroral oval, *Rev. Geophys.*, *45*, RG1003, doi:10.1029/2005RG000174.

Frey, H. U., S. B. Mende, T. J. Immel, J.-C. Gérard, B. Hubert, S. Habraken, J. Spann, G. R. Gladstone, D. V. Bisikalo, and V. I. Shematovich (2003), Summary of quantitative interpretation of image far ultraviolet auroral data, *Space Sci. Rev.*, *109*, 255–283, doi:10.1023/B:SPAC.0000007521.39348.a5.

Frey, H. U., G. Haerendel, S. B. Mende, W. T. Forrester, T. J. Immel, and N. Ostgaard (2004), Subauroral morning proton spots (SAMPS) as a result of plasmapause-ring-current interaction, *J. Geophys. Res.*, *109*, A10305, doi:10.1029/2004JA010516.

Fukunishi, H. (1969), Occurrences of sweepers in the evening sector following the onset of magnetospheric substorms, *Rep. Ionos. Space Res. Jpn.*, *23*, 21–34.

Fukunishi, H., T. Toya, K. Koike, M. Kuwashima, and M. Kawamura (1981), Classification of hydromagnetic emission based on frequency-time spectra, *J. Geophys. Res.*, *86*, 9029–9039, doi:10.1029/JA086iA11p09029.

Fuselier, S. A., S. P. Gary, M. F. Thomsen, E. S. Claflin, B. Hubert, B. R. Sandel, and T. Immel (2004), Generation of transient dayside subauroral proton precipitation, *J. Geophys. Res.*, *109*, A12227, doi:10.1029/2004JA010393.

Gendrin, R. (1970), Substorm aspects of magnetic pulsations, *Space Sci. Rev.*, *11*, 54–130, doi:10.1007/BF00174429.

Hansen, H. J., B. J. Fraser, F. W. Menk, and R. E. Erlandson (1995), Ground satellite observations of Pc1 magnetic pulsations in the plasma trough, *J. Geophys. Res.*, *100*, 7971–7985, doi:10.1029/94JA02576.

Heacock, R. R. (1967), Evening micropulsation events with a rising mid-frequency characteristics, *J. Geophys. Res.*, *72*, 399–408, doi:10.1029/JZ072i001p00399.

Hubert, B., J.-C. Gérard, S. A. Fuselier, and S. B. Mende (2003), Observation of dayside subauroral proton flashes with the IMAGE-FUV imagers, *Geophys. Res. Lett.*, *30*(3), 1145, doi:10.1029/2002GL016464.

Immel, T. J., S. B. Mende, H. U. Frey, L. M. Peticolas, C. W. Carlson, J.-C. Gérard, B. Hubert, S. A. Fuselier, and J. L. Burch (2002), Precipitation of auroral protons in detached arc, *Geophys. Res. Lett.*, *29*(11), 1519, doi:10.1029/2001GL013847.

Immel, T. J., S. B. Mende, H. U. Frey, J. Patel, J. W. Bonnell, M. J. Engebretson, and S. A. Fuselier (2005), ULF waves associated with enhanced subauroral proton precipitation, in *Inner Magnetosphere Interactions: New Perspectives From Imaging*, *Geophys. Monogr. Ser.*, vol. 159, edited by J. L. Burch, M. Schulz, and H. Spence, pp. 71–84, AGU, Washington, D. C.

Jordanova, V. K., M. Spasojevic, and M. F. Thomsen (2007), Modeling the electromagnetic ion cyclotron wave-induced formation of detached subauroral proton arcs, *J. Geophys. Res.*, *112*, A08209, doi:10.1029/2006JA012215.

Kangas, J., A. Guglielmi, and O. Pokhotelov (1998), Morphology and physics of short-period magnetic pulsations (a review), *Space Sci. Rev.*, *83*, 435–512, doi:10.1023/A:1005063911643.

Khazanov, G. V., K. V. Gamayunov, D. L. Gallagher, J. U. Kozyra, and M. W. Liemohn (2007), Self-consistent model of magnetospheric ring current and propagating electromagnetic ion cyclotron waves: 2. Wave-induced ring current precipitation and thermal electron heating, *J. Geophys. Res.*, *112*, A04209, doi:10.1029/2006JA012033.

Kiselev, B. V., and O. M. Raspopov (1971), Frequency drift of geomagnetic pulsations of the IPDP type (in Russian), *Geomagn. Aeron.*, *11*, 731–734.

Kozyra, J. U., V. K. Jordanova, R. B. Horne, and R. M. Thorne (1997), Modeling of the contribution of electromagnetic ion cyclotron (EMIC) waves to stormtime ring current erosion, in *Magnetic Storms*, *Geophys. Monogr. Ser.*, vol. 98, edited by B. T. Tsurutani et al., pp. 187–202, AGU, Washington, D. C.

Lin, C. S., and G. K. Parks (1976), Ion cyclotron instability of drifting plasma clouds, *J. Geophys. Res.*, *81*, 3919–3922, doi:10.1029/JA081i022p03919.

Maltseva, N. F., A. V. Gul'elmi, and V. A. Vinogradova (1970), Effect of the westward frequency drift in the intervals of pulsations with decreasing period (in Russian), *Geomagn. Aeron.*, *10*, 939–941.

Maltseva, N., V. Troitskaya, E. Gerazimovitch, L. Baransky, S. Asheim, J. Holtet, K. Aasen, A. Egeland, and J. Kangas (1981), On temporal and spatial development of IPDP source region, *J. Atmos. Terr. Phys.*, *43*, 1175–1188, doi:10.1016/0021-9169(81)90033-7.

Mende, S. B., et al. (2000), Far ultraviolet imaging from the IMAGE spacecraft. 1. System design, *Space Sci. Rev.*, *91*, 243–270, doi:10.1023/A:1005271728567.

Pikkarainen, T., J. Kangas, B. Kiselev, N. Maltseva, R. Rakhmatulin, and S. Solovjev (1983), Type IPDP magnetic pulsations and the development of their sources, *J. Geophys. Res.*, *88*, 6204–6212, doi:10.1029/JA088iA08p06204.

Søraas, F., J. Å. Lundblad, N. F. Maltseva, V. A. Troitskaya, and V. Selivanov (1980), A comparison between simultaneous IPDP groundbased observations of energetic protons obtained by satellites, *Planet. Space Sci.*, *28*, 387–405, doi:10.1016/0032-0633(80)90043-4.

Spasojević, M., H. U. Frey, M. F. Thomsen, S. A. Fuselier, S. P. Gary, B. R. Sandel, and U. S. Inan (2004), The link between a detached subauroral proton arc and a plasmaspheric plume, *Geophys. Res. Lett.*, *31*, L04803, doi:10.1029/2003GL018389.

Spasojević, M., M. F. Thomsen, P. J. Chi, and B. R. Sandel (2005), Afternoon subauroral proton precipitation resulting from ring current–plasmasphere interaction, in *Inner Magnetosphere Interactions: New Perspectives From Imaging*, *Geophys. Monogr. Ser.*, vol. 159, edited by J. Burch, M. Schulz, and H. Spence, pp. 85–100, AGU, Washington, D. C.

Trakhtengerts, V. Y., and A. G. Demekhov (2005), Discussion paper: Partial ring current and polarization jet, *Int. J. Geomagn. Aeron.*, *5*, GI3007, doi:10.1029/2004GI000091.

Troitskaya, V. A., R. V. Schepetnov, and A. V. Gulyel'mi (1968), Estimates of electric fields in the magnetosphere from the frequency drift of micropulsations, *Geomagn. Aeron.*, Engl. Transl., *8*, 794–795.

Yahnin, A. G., T. A. Yahnina, and H. U. Frey (2007), Subauroral proton spots visualize the Pc1 source, *J. Geophys. Res.*, *112*, A10223, doi:10.1029/2007JA012501.

Yahnin, A. G., T. A. Yahnina, and H. U. Frey (2008), Identification of sources of Pc1 geomagnetic pulsations on the basis of proton aurora observations, *Cosmic Res.*, Engl. Transl., *46*, 335–338, doi:10.1134/S0010952508040084.

Yahnina, T. A., A. G. Yahnin, J. Kangas, J. Manninen, D. S. Evans, A. G. Demekhov, V. Y. Trakhtengerts, M. F. Thomsen, G. D. Reeves, and B. B. Gvozdevsky (2003), Energetic particle counterparts for geomagnetic pulsations of Pc1 and IPDP types, *Ann. Geophys.*, *21*, 2281–2292.

Yahnina, T. A., H. U. Frey, T. Bösinger, and A. G. Yahnin (2008), Evidence for subauroral proton flashes on the dayside as the result of the ion cyclotron interaction, *J. Geophys. Res.*, *113*, A07209, doi:10.1029/2008JA013099.

Zhang, Y., L. J. Paxton, T. J. Immel, H. U. Frey, and S. B. Mende (2002), Sudden solar wind dynamic pressure enhancements and dayside detached auroras: IMAGE and DMSP observations, *J. Geophys. Res.*, *107*, 8001, doi:10.1029/2002JA009355. [Printed *108*(A4), 2003.]

Zhang, Y., L. J. Paxton, and Y. Zheng (2008), Interplanetary shock induced ring current auroras, *J. Geophys. Res.*, *113*, A01212, doi:10.1029/2007JA012554.

T. Bösinger, Department of Physical Sciences, University of Oulu, FI-90014, Oulu, Finland.

H. U. Frey, Space Sciences Laboratory, University of California, Berkeley, CA 94720, USA.

J. Manninen, Sodankylä Geophysical Observatory, Tähteläntie 62, FI-99600, Sodankylä, Finland.

A. G. Yahnin and T. A. Yahnina, Polar Geophysical Institute, Kola Science Centre, Russian Academy of Science, Apatity, Murmansk Oblast, 184200, Russia. (yahnin@pgia.ru)